



AIAA 2000-5136
Exploration of the Design Space for the
***ABL*V-GT SSTO Reusable Launch Vehicle**

J. Bradford
J. Olds
R. Bechtel
T. Cormier
Georgia Institute of Technology
Atlanta, GA

D. Messitt
Aerojet Propulsion Division
Sacramento, CA

AIAA Space 2000 Conference and Exposition
19-21 September 2000
Long Beach, California

Exploration of the Design Space for the *ABLV-GT* SSTO Reusable Launch Vehicle

John Bradford[†], John R. Olds^{††}, Ryan Bechtel[†], Tim Cormier[†]
 Space Systems Design Laboratory
 School of Aerospace Engineering
 Georgia Institute of Technology, Atlanta, GA

Donald G. Messitt^{*}
 Aerojet Propulsion Division
 Sacramento, CA

ABSTRACT

The *ABLV-GT* is a conceptual design for an advanced reusable launch vehicle based on the current NASA Langley ABLV concept. It is a Vision Vehicle class, horizontal takeoff, horizontal landing single-stage-to-orbit vehicle. Main propulsion is provided by Aerojet's 'Strutjet' LOX/LH2 rocket-based combined cycle engine design. The *ABLV-GT* is designed to deliver 25,000 lbs. to the orbit of the International Space Station from Kennedy Space Center.

This paper will report the findings of a conceptual design study on the *ABLV-GT* performed over the last year by members of the Space Systems Design Lab at Georgia Tech. This work has been sponsored by the Advanced Reusable Transportation Technologies program office at NASA Marshall Space Flight Center.

Details of the concept design including external and internal configuration, mass properties, trajectory analysis, aerodynamics, and aeroheating are given.

[†] - Graduate Research Assistant, School of Aerospace Engineering, Student member AIAA.

^{††} - Assistant Professor, School of Aerospace Engineering, Senior member AIAA.

^{*} - Aerojet Hypersonic Propulsion Products, Member AIAA.

Copyright ©2000 by John E. Bradford, John R. Olds and Donald G. Messitt. Published by the American Institute of Aeronautics and Astronautics, Inc. with permission.

This vehicle study resulted in the closure of 18 different vehicle designs. The trade variables included air-breathing transition Mach number, mechanical versus thermal choke engine, and payload weight. Initial results for a vehicle with a turbine-powered low-speed propulsion system were generated and will be presented. Finally, a low earth orbit concept with a reduced payload weight will be shown.

NOMENCLATURE

AAR	air augmented rocket
ABLV	air-breathing launch vehicle
C_t	thrust coefficient ($T/q/A_{ref}$)
DMRJ	dual mode ramjet
EMA	electromechanical actuator
ESJ	ejector scramjet
I_{sp}	specific impulse (sec.)
I^*	equivalent trajectory averaged I_{sp} (sec.)
ISS	international space station
KSC	Kennedy Space Center
LEO	low earth orbit
LH2	liquid hydrogen
LOX	liquid oxygen
MR	mass ratio (gross weight/burnout weight)
OML	outer mold line
OMS	orbital maneuvering system
PEF	packaging efficiency factor
q	dynamic pressure (psf)
RBCC	rocket based combined-cycle
RCS	reaction control system
T/W	vehicle thrust-to-weight at takeoff
T/W_e	installed engine thrust-to-weight at sls
TPS	thermal protection system

INTRODUCTION

NASA Marshall Space Flight Center is currently conducting a ground test program to evaluate rocket-based combined cycle (RBCC) engines. These multi-mode engines combine the best aspects of rocket propulsion (high thrust-to-weight) and airbreathing propulsion (high I_{sp}). Previous research has shown that vehicles utilizing RBCC propulsion have the potential to be attractive candidates for future space launch missions^{1,2}.

As part of its Advanced Reusable Technologies program, NASA conducted vehicle-level system studies³. The studies involved comparison of different RBCC and turbine-based combination propulsion systems using data provided by various engine contractors. The vehicle configuration was derived from the current Langley Research Center (LaRC) 2-D airframe integrated scramjet design⁴.

The ABLV, which stands for Air-Breathing Launch Vehicle, is designed to deliver 25,000 lbs to the International Space Station, at an altitude of 220 nmi. and inclination of 51.6 degrees. The reference concept is an unpowered, single stage vehicle that takes off and lands horizontally. The propellants are triple point hydrogen and liquid oxygen. Advanced TPS and structural materials are assumed in the design.



Figure 1. Hyper-X Test Vehicle.

The Hyper-X vehicle (see figure 1) uses an external mold-line shape similar to the full-scale ABLV reference concept. Hyper-X is a 1/16 scale flight vehicle that will demonstrate scramjet engine

operation in the Mach 7 and Mach 10 flight regime and provide flight data for code calibration⁵. Additionally, aerodynamic data will also be obtained from the test flight for verification of wind tunnel results.

REFERENCE CONCEPT

The *ABLV-GT* was largely based on the reference concept, which is referred to as the ABLV-4 or ABLV-9, depending upon the type of low-speed engine system. This particular vehicle design has been under study since the early 1980's. Small design changes have been made over the years and this concept is considered by LaRC to be highly evolved and optimized.

The vehicle forebody consists of multiple ramps, starting with a 6° turn angle and progressing towards a final turn angle around 11° measured with respect to the vehicle centerline. The main propulsion system has three separate components: a low-speed system, a high-speed dual-mode scramjet system, and a tail rocket system.

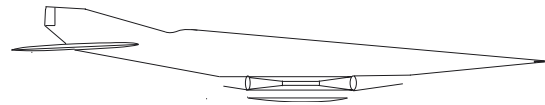


Figure 2. Over-Under Propulsion System.

For the Mach 0 to 3 range, the low-speed turbine system on the ABLV-9, named ACE-TR (Air-Core Enhanced TurboRamjet), provides the majority of the thrust at takeoff, through transonic flight, and up to ramjet takeover speeds. This low speed system is composed of 6-8 separate turbojet-like engines and are arranged in an over-under configuration with the high-speed engine system. During ACE-TR operation, a portion of the vehicle forebody compression ramps are actuated downward to provide air intake to these engines. Above Mach 3, the forebody inlet ramps are closed, protecting the low-speed system and providing the inlet flowfield and mass capture requirements for the high-speed system. Figure 2 shows the over-under arrangement of this system.

A linear aerospike rocket engine, in the aft section of the vehicle, provides additional thrust at takeoff, through the transonic pinch point, and in the final stages of orbital insertion. From Mach 3 to Mach 18, the system utilizes the dual-mode ramjet propulsion system, with LOX augmentation occurring at the higher scramjet Mach numbers. The engine geometry is highly variable with an adjustable cowl lip to keep the engine operating close to its design point.

From Mach 18 to orbital injection at 30 nmi. by 100 nmi., the linear aerospike is used again. The aerospike engine is also used for orbit transfer maneuvers to obtain the final circular space station orbit and for the deorbit burn.

The ‘wings’ attached to the aft section of the fuselage are all-moving horizontal control surfaces and are not used to generate lift during takeoff. Vertical control surfaces, ‘tails’, are located directly above the wings on the fuselage. Large hydraulic actuators are required to move these surfaces during flight.

The ABLV-4 and 9 use a number of advanced technologies in addition to the propulsion systems. Graphite composites are used to construct the 5 psig triple-point hydrogen propellant tanks. Aluminum-Lithium (Al-Li) is used for the multi-lobed oxygen tank. Active cooling is required on the vehicle nose, leading edge, and forebody. Additionally, lightweight power, avionics, and landing gear are assumed. The vehicle is capable of autonomous operation and thus requires no pilots. Initial operational capability (IOC) is expected to be in the year 2020 – 2025.

COLLABORATIVE DESIGN PROCESS

The *ABLV-GT* was designed using a collaborative, team-oriented approach in the Space Systems Design Lab (SSDL) at Georgia Tech and Aerojet’s Propulsion Division. An integrated design team of disciplinary experts was assembled. Each team member used a conceptual design tool to conduct his or her engineering analysis in a highly coupled and iterative concept convergence process similar to that described in reference 2. Table 1 lists the represented engineering disciplines and the conceptual design tools used by analysts in each.

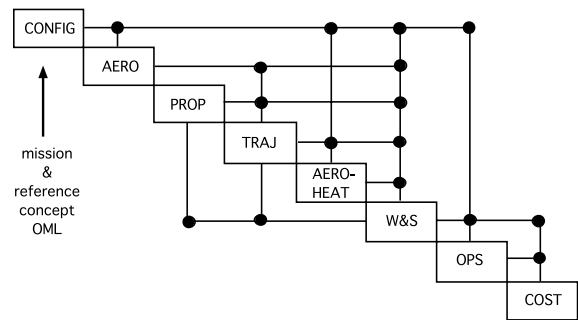


Figure 3. *ABLV-GT* Design Structure Matrix.

Table 1. Disciplinary Representation.

Discipline	Analysis Tool
CAD and Layout	SDRC I-DEAS
Aerodynamics	APAS (UDP, HABP)
RBCC Propulsion	various
TBCC Propulsion	GECAT
Trajectory	POST (3-D)
Aeroheating/TPS	MINIVER/TCAT
Weights & Sizing	in-house spreadsheet
Ground Operations	AATe
Cost and Economics	CABAM

Data was exchanged between the team members according to the coupling links in the Design Structure Matrix (DSM, figure 3). In the DSM, the data links above the diagonal represent feed forward data from one analyst to a subsequent analyst. Feedback links below the diagonal represent iteration loops for which an initial guess must be made and then iteration performed to converge the results of the two disciplines. For example, a strong iteration loop is present between propulsion, performance (trajectory optimization), and mass properties (weights & sizing). As the vehicle size and capture area changes, the engine performance must be updated and the trajectory re-optimized. During the conceptual design process, the convergence tolerance was taken to be a change of less than 0.1% in gross weight between iterations.

ABLV-GT MODEL

In order to establish a RBCC version of the ABLV reference concept, a number of modifications were required. In addition to accommodating Aerojet's engines and keel line, changes were made to improve vehicle operability in the areas of TPS, OMS, and actuators. A brief discussion of each disciplines' modeling process, assumptions, and changes to the reference design will be provided next.

Mission Profile

The *ABLV-GT* operates from a notional airfield at KSC. The vehicle is designed for a nominal thrust-to-weight ratio of 0.6 during takeoff. The vehicle accelerates onto a 2,100 psf dynamic pressure boundary at Mach 2.5, where the ramjet engines can be used (inlet is started). The vehicle initially injects to a 30x100 nmi. orbit at 51.6° inclination. The vehicle coasts to apogee position and the OMS engines are ignited to circularize the vehicle into a 100 nmi. ISS phasing orbit. At the appropriate orbital position, the OMS engines are refired two more times, once to transfer to 100x220 nmi. elliptical orbit, then to the final 220 nmi. circular orbit. The total delta-V requirement for these three maneuvers is estimated to be about 400 fps. Upon docking with the ISS, the payload is released and the vehicle is de-orbited for the return to KSC. A deorbit delta-V capability of 350 fps is allotted. Figure 4 provides a pictorial overview of the entire mission.

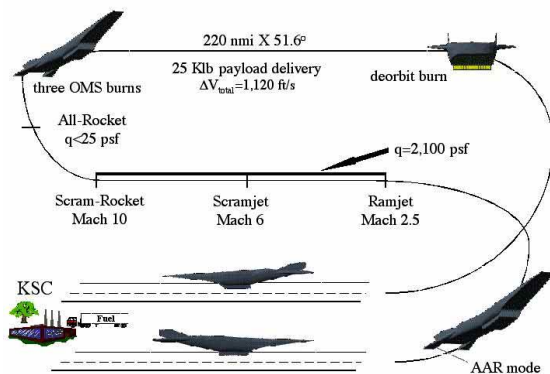


Figure 4. *ABLV-GT* Mission Profile.

Internal Configuration & Layout (CAD)

A fuselage outer mold line (OML) representative of the LaRC configuration was created using SDRC I-DEAS, a solid modeling program. Propellant tanks were packaged in the fuselage of the vehicle, at an initially assumed LOX/LH2 mixture ratio of 2.2 (by weight).

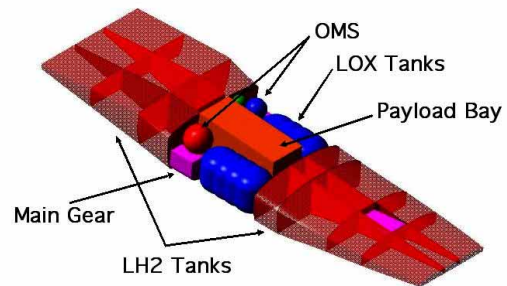


Figure 5. Internal CAD Arrangement.

As shown in Figure 5, a transparent view of the fuselage, the fore and aft vehicle volumes are occupied by LH2 tanks. These tanks are integral, that is, they share a common wall with the airframe where possible. A 15 ft. x 15 ft. x 35 ft. cargo bay was reserved for the 25,000 payload. This is a slightly larger payload than the reference concept, but the additional volume allows for up to 18 passengers to be transported. Two non-integral, multi-lobed LOX tanks hold the required oxidizer and are located adjacent to the payload bay. Note that this internal tank arrangement is different than the Langley reference. In the Langley configuration, the LOX tanks are located in the nose and tail sections of the vehicle. For the *ABLV-GT*, with its inherently higher mixture ratio, placing the dense LOX tanks in the center of the fuselage will reduce the bending loads on the vehicle. Separate spherical tanks adjacent to the payload bay contain the OMS propellants. Storage compartments for the main and nose landing gear are also present in the model. Additionally, small helium, gaseous hydrogen (GH2), and gaseous oxygen (GOX) tanks for the RCS are located in the nose and tail sections of the vehicle.

One of the key outputs of the CAD discipline is the fraction of total internal fuselage volume that is occupied by ascent propellants (propellant packaging efficiency, PEF). Since the tank configuration changes slightly with vehicle scale (payload volume is fixed), three different internal layouts were created — one each at three different vehicle length scales of 85%, 100%, and 115% of the “as drawn” vehicle. A 1-D curve was created to allow interpolation between the points on the curve. As an example, the converged baseline vehicle length was 190.5 feet tip-to-tail, which corresponded to a PEF of 70.8%.

Aerodynamics

The external fuselage configuration of the *ABLVT* was based on the reference concept. The forebody design was changed to reflect the Strutjet engine’s Mach 6/10 forebody design. This forebody design begins with a 6° compression ramp. A series of nearly isentropic ramps (angles $< 1^\circ$) are then used to achieve the desired 18° final turn angle. At Mach 6, all of the weaker secondary shocks are focused on the cowl lip. At Mach 10, the bow shock will be focused on the cowl lip and the secondary shocks will be inside the inlet (see figure 6). The aftbody nozzle was shaped to provide a large expansion area for scramjet and all-rocket modes of operation.

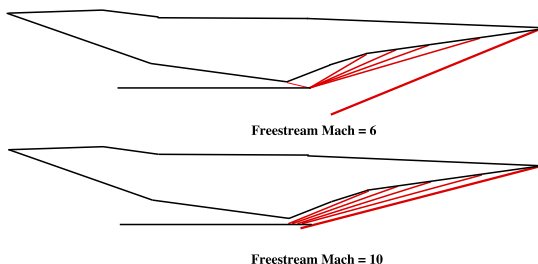


Figure 6. Mach 6/10 Forebody Design Keel Line.

An aerodynamic database consisting of tables with lift and drag coefficients were generated across the ascent trajectory speed and altitude regime using APAS⁶. At each Mach number and altitude combination of interest, analysis was performed over a range of angles-of-attack (AOA) from -10° to 20° , in 5° increments. For all cases, the ‘wings’ were at zero incidence with respect to the vehicle centerline. These data tables were then provided to the trajectory analyst.

Subsequent vehicle scaling was done photographically and the aerodynamic coefficients were assumed to remain constant during scaling. The aerodynamic analysis was therefore only required at the start of the design process. Note that in the force accounting system used, all forebody and upper surface pressures were included as aerodynamic drag and the propulsive force was taken to be from the cowl lip to the tail of the vehicle (cowl-to-tail system). It should be noted that for convenience, the drag from the engine struts extending upstream of the cowl lip were also included in the propulsive force calculation.

The aerodynamic tables for the supersonic flight regime were generated using HABP-Hypersonic Arbitrary Body Program. Subsonic lift and drag coefficients were extrapolated from the supersonic values. The fuselage was analyzed using ‘tangent-cone empirical’ for the impact method and ‘Prandtl-Meyer empirical’ for the shadow method. The pressure coefficient for the base was set to zero to account for the engine coupling. The values for $Re-\theta/\text{Mach}$ parameter for the momentum thickness boundary layer transition method was set to 150 and 350 for axis-symmetric and 2-D flow respectively.

Figure 7 shows an off-center, banked view of the vehicle model generated in APAS for use in the analysis. Note that the wings are not connected to the actual vehicle. Because APAS is not actually resolving the complex flowfield around the vehicle and is using local surface inclination methods, the disconnect does not affect the results (fuselage and wing additive).

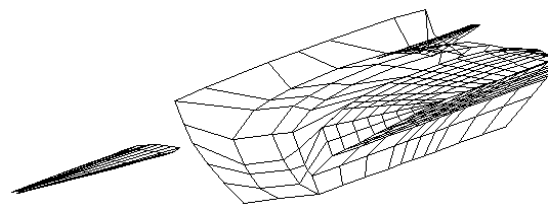


Figure 7. APAS Model.

Propulsion

The *ABLVT* main propulsion system uses two liquid oxygen and hydrogen ejector scramjet (ESJ) Strutjet RBCC engines to inject the vehicle into a 30

nmi. by 100 nmi. interim transfer orbit. The vehicle consists of two engines, each with 8 struts (total of 16). The struts provide 3-D flow compression, structural integrity, and housing for the rocket subsystems. Figure 8 shows this unique engine concept. More details on the performance capability and physical design can be found in references 7 and 8.

A LOX/LH₂ rocket primary with a chamber pressure of 2,000 psi and mixture ratio of 7.0 was selected. The all-rocket performance calculations use the same rocket primary subsystem from the AAR mode, but with a significantly higher expansion ratio (ϵ).

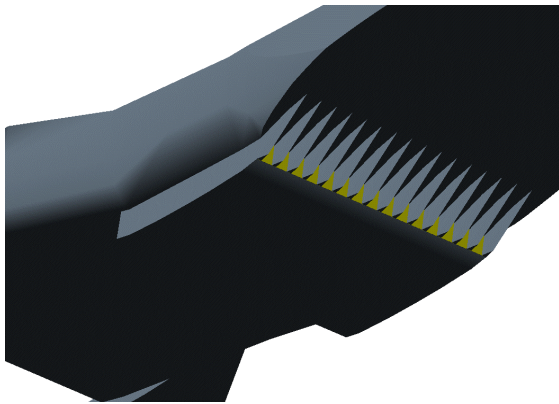


Figure 8. Aerojet's Strutjet Engine.

Using the full Strutjet engine dataset generated by Aerojet, a tabular engine deck suitable for use in the trajectory simulation was created in a spreadsheet. This spreadsheet allowed for quick scaling and updating of the engine data. The deck includes engine thrust, thrust coefficient (C_t), and I_{sp} for a range of altitudes, Mach numbers, and angles of attack (AOA) for each operating mode. Due to numerical difficulties in the trajectory simulation, the ramjet and scramjet mode AOA data is at a single, averaged value for each mode. This value was adjusted during the vehicle closure to coincide with the flight AOA. It should also be noted that the engines were scaled based on the vehicle scale factor (SF) squared, where the scale factor is the vehicle length over the reference length (L/L_{ref}). In scaling the engines in this manner, the vehicle takeoff T/W varied from the nominal value of 0.6 during the closure process.

Performance (Trajectory Optimization)

The trajectory analysis was performed by the three degree-of-freedom version of the Program to Optimize Simulated Trajectories—POST⁹. POST is a Lockheed Martin and NASA code that is widely used for trajectory optimization problems in advanced vehicle design. It is a generalized event-oriented code that numerically integrates the equations of motion of a flight vehicle given definitions of aerodynamic coefficients, propulsion system characteristics, and a weight model. Numerical optimization is used to satisfy trajectory constraints and minimize a user-defined objective function. The objective of the trajectory is to maximize the final weight, or burnout weight.

The trajectory for the *ABLVT* is constrained by a dynamic pressure boundary, changes in pitch rates that provide smooth AAR and rocket pull-ups, and by orbital termination criteria. The dynamic pressure boundary flown is 2,100 psf during ramjet and scramjet modes (Mach 2.5 to Mach 10). The q boundary is constrained through implementation of a linear feedback control guidance scheme in which the dynamic pressure is held constant by controlling angle-of-attack.¹⁰ For the baseline case above Mach 10, the vehicle begins to pull up and the q -boundary constraint is no longer enforced. During the pull-up, the rockets in the flowpath are reignited, the inlets remain open, and the engines operate in 'scram-rocket' mode. This transition to all-rocket mode is complete by approximately Mach 13. The *ABLVT* flies to an optimal MECO condition such that the apogee altitude is 100 nmi. at an inclination of 51.6°. A minimum perigee constraint of 30 nmi. is also specified. A separate OMS propulsion system is used to circularize the orbit at 100 nmi., transfer to 220 nmi., and later deorbit the vehicle. The baseline LOX/LH₂ OMS is designed to deliver 1,120 fps of on-orbit ΔV . A 400 fps ΔV budget for ISS rendezvous and operations is included in the OMS budget of 1,120 fps.

Aerothermal Analysis

For the *ABL**V-GT*, a lightweight blanket system, TABI, is used for the leeward fuselage surface. MINIVER¹¹ and T-CAT¹² were used to determine the required thickness of the blankets based on the vehicle's flown trajectory. Since the exposed wing is constructed of a high-temperature titanium-aluminide (Ti-Al), large sections of the wing are designed to be hot structure. To avoid the complexities of active cooling present on the reference concept, an ultra-high temperature ceramic (UHTC) is employed on the small radius nose and wing leading edges. This material is being developed by NASA – Ames and is capable of withstanding temperatures as high as 4,500° F. Additional information about the various types of advanced thermal protection system (TPS) materials selected can be found in reference 12 and 13.

For the forebody ramp TPS, a unique LaRC designed C/SiC tile with multi-layer insulation (MLI), platinum, and gold plating was used. A structural unit weight of 1.59 psf, provided in a previous paper on the reference concept, was assumed for these areas.⁴

Mass Properties

A three-level spreadsheet model consisting of approximately 75 parametric mass estimating relationships (MER's) was created to estimate the weight and size of the converged *ABL**V-GT* vehicle. For example, MER's were included that estimate the wing weight based on surface area and wing loading, the fuselage MER was based on a smeared unit weight of 2.5 psf, and the landing gear weight was estimated as 2.5% of the GLOW (gross liftoff weight). Aerojet provided the value for the installed T/W₀ of the Stutjet engine. This number depended upon design variables such as number of struts, ramjet dynamic pressure, scramjet dynamic pressure, and transition Mach number.

Given a MR (or propellant mass fraction) and a mixture ratio requirement from the trajectory optimization simulation, the spreadsheet was used to scale the vehicle up or down until the available MR matched that required. The changing PEF was also accounted for during this process. The engine T/W was fixed during the scaling process. Once the vehicle was

“closed” within the Weights & Sizing discipline, the results were sent back to the Propulsion discipline to resize the engines, and then to the Trajectory discipline to reoptimize the vehicle trajectory with the new size, weight, and engine performance. Between 10 and 15 iterations around the Propulsion – Trajectory - Weights loop, shown in the DSM in Fig. 4, are required to obtain convergence. This entire process was repeated until the change in gross weight between successive iterations was converged to within 0.1%.

BASELINE *ABL**V-GT* RESULTS

The baseline *ABL**V-GT* design has a gross weight of 1,352,000 lb. and a dry weight of 230,000 lb. The fuselage length is 190.5 ft. from tip to tail, with a wingspan of 86 feet. Table 2 lists selected summary items from the weight breakdown structure (WBS). The full WBS is not included in this paper for brevity, but includes 28 major headings with several subcategories under each. A lumped 15% overall dry weight growth margin was included to account for the likelihood of weight increases.

Table 2. *ABL**V-GT* Top-Level Weight Statement.

WBS Item	Weight
Wing & Tail Group	36,575 lb.
Fuselage and LOX Tanks	62,950 lb.
Thermal Protection System	17,450 lb.
Propulsion (main, OMS, RCS)	45,515 lb.
Subsystems & Other Dry Weights	37,525 lb.
Dry Weight Margin (15%)	<u>30,000 lb.</u>
Dry Weight	230,000 lb.
Payload to ISS	25,000 lb.
Other Inert Weights	<u>36,575 lb.</u>
Insertion Weight	291,575 lb.
LH2 Ascent Propellant	233,975 lb.
LOX Ascent Propellant	<u>826,450 lb.</u>
Gross Weight	1,352,000 lb.

For the converged baseline, the Mass Ratio (MR) of the ascent was determined to be 4.64, with an ascent mixture ratio (no OMS propellants) of 3.54. The ideal ascent ΔV provided by the propulsion system is

34,755 fps, including 7,950 fps of drag losses (measured in the inertial frame). Therefore, the I^* for the ascent is estimated to be 496 sec.

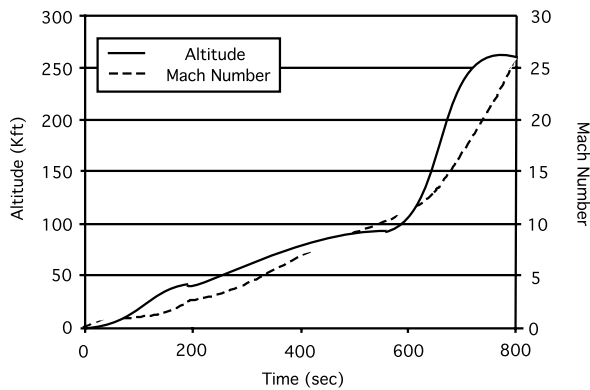


Figure 9. Altitude and Mach Number vs Time.

Figure 9 shows a graph of Altitude and Mach number versus time. A plot of the dynamic pressure as a function of Mach number is given in Figure 10. The 2,100 psf q-boundary can clearly be seen in the figure. The linear feedback control algorithm quickly guides the vehicle to the boundary. The angle-of-attack profile for the entire trajectory can be seen in Figure 11. The dynamic pressure is held between ~205 seconds and ~575 seconds. The Mach number transitions between the four engine modes (AAR, Mach 0 – Mach 2.5; ramjet, Mach 2.5 – Mach 6; scramjet, Mach 6 – Mach 10; scram-rocket, Mach 10 – Mach ~13; and rocket, Mach 13 – orbit insertion) are modeled as a linear ramp down of the preceding mode and a linear ramp up of the following mode, over a 0.2 Mach number increment. Scram-rocket mode termination is optimized by POST and constrained so operation below a dynamic pressure of 25 psf does not occur.

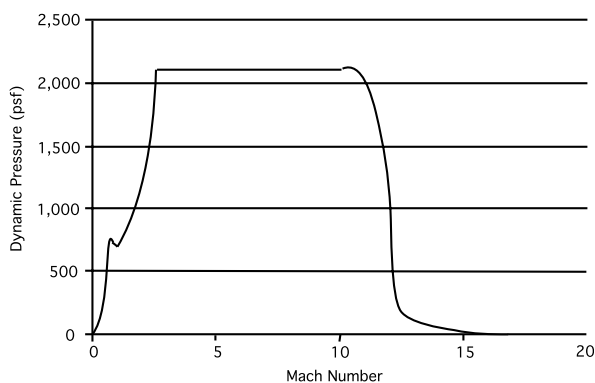


Figure 10. Dynamic Pressure vs Mach Number.

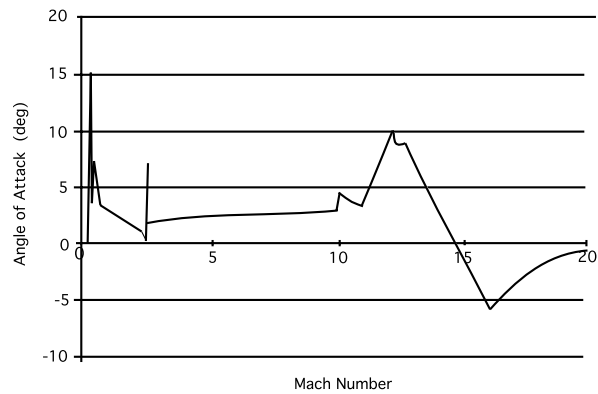


Figure 11. Angle of Attack vs Mach Number.

The drag coefficient (C_d) versus Mach number is presented in Figure 12. The *ABL*V-GT's theoretical wing area (S_{ref}) was used for normalizing the drag values. It should also be mentioned that the drag at Mach 1 was estimated as a factor of 1.5 higher than the drag at Mach 2, generated by APAS.

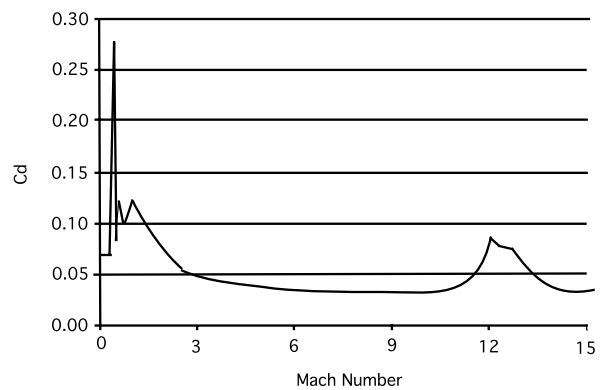


Figure 12. Drag Coefficient vs Mach Number.

TRADE STUDIES

Transition Mach Number

A sweep of the scramjet transition Mach number (M_{tr}) was conducted from Mach 10 to Mach 13 for the *ABL*V-GT configuration with the Mach 6/10 forebody design. Note that the engine is oversped above Mach 10. Due to the harsher flight environment (increased heating, internal bow shock, etc.), the engine weight will increase with transition Mach number. Additionally, the TPS thicknesses are required to be increased.

Aerojet provided the engine T/W for each new transition Mach number. On average, for each Mach number increment, the T/W_e decreased by ~ 1%. MINIVER and TCAT were rerun for the higher transition Mach number cases to provide new TABI unit weights. The forebody, C/SiC TPS unit weights were unchanged from the previous values.

Table 3. Strutjet Transition Mach Number Trade Results.

M_{tr}	GLOW (Klbs)	Dry (Klbs)	Mix. Ratio	Length (ft)
10	1,352	230	3.54	190.5
11	1,290	229	3.17	190.9
12	1,374	252	2.70	199.5
13	1,722	312	2.12	221.0

Table 3 provides a summary of the converged vehicle parameters of interest. Note the significant drop in mixture ratio with increasing flight Mach number. While this helped to reduce the weight of vehicle systems like the landing gear, the drag rise due to the larger vehicle (more low-density LH2 onboard), increased TPS weight, reduced engine performance, and lower engine weight eventually dominated the overall performance. This is evident in the sharp increase in dry weight and GLOW from Mach 12 to 13.

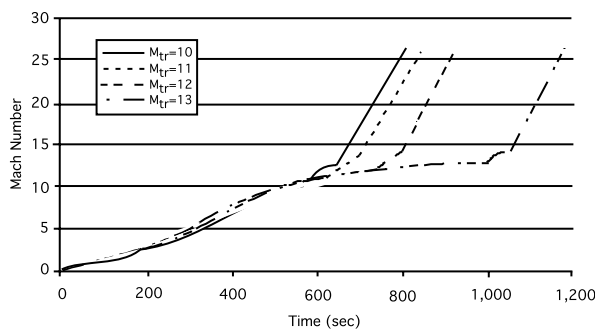


Figure 13. Mach Number vs Time.

Figures 13 and 14 show the trajectory plots of Mach number versus time and dynamic pressure versus Mach number. Note the significant increase in ascent time that the vehicle takes to accelerate from Mach 13 from 12, compared to Mach 11 from 10. This is due to the quickly degrading oversped engine performance for

the Mach 6/10 forebody design point. Figure 14 clearly shows that for each case, the 2,100 psf q boundary is being held until their respective transition Mach number is reached.

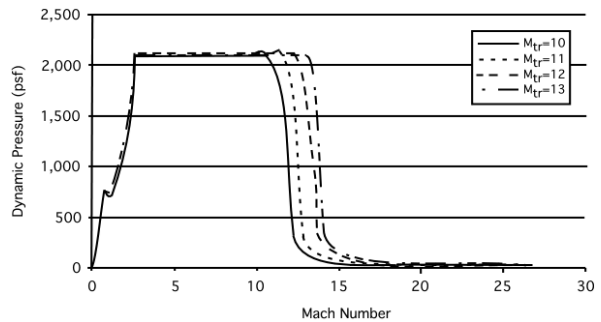


Figure 14. Dynamic Pressure vs Mach number.

From these results, it appears that a weight minimum is occurring between the Mach 10 and Mach 12 point, with the GLOW and dry weight growing very quickly above Mach 12.

Engine Type Trade

As an alternative to the baseline, the Strutjet engine system was replaced with a Dual-Mode Ramjet (DMRJ) version. This engine features a significantly higher thrust-to-weight ratio (20-30%), but lower performance in AAR and ramjet modes. The engine design is simplified by elimination of the mechanical choke downstream of the combustor, in favor of a thermal choke. This thermal choke is accomplished through a more sophisticated fuel injection scheme. Scramjet, scram-rocket, and all-rocket mode performance is identical to the baseline engine performance.

Table 4. DMRJ Transition Mach Number Trade Results.

M_{tr}	GLOW (Klbs)	Dry (Klbs)	Mix. Ratio	Length (ft)
10	1,287	207	3.65	187.3
11	1,248	208	3.26	188.8
12	1,347	260	2.83	197.8
13	1,687	284	2.28	218.4

As before, Aerojet provided the engine performance data and weight for the DMRJ engines. The same sweep of scramjet transition Mach numbers performed for the Strutjet engine was then performed for the DMRJ engine configuration.

Table 4 provides a results summary for the DMRJ cases. Figure 15 provides a comparison of GLOW and dry weights for both the Strutjet and DMRJ engines. From these results, it is clear that based on a vehicle weight metric, the benefits of the lower engine weight outweigh the decrease in engine performance in AAR and ramjet modes. Both the Strutjet and DMRJ appear to reach their minimum GLOW and dry weight near Mach 11. The Mach 11 DMRJ vehicle represents an improvement of 10% in dry weight and 8% in GLOW, compared to the baseline Mach 10 transition Strutjet.

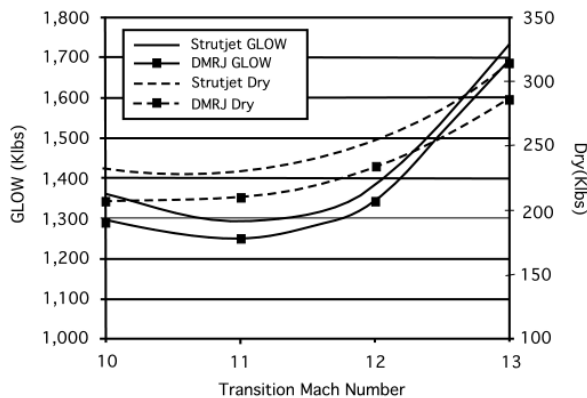


Figure 15. Strutjet and DMRJ M_{tr} Results.

Payload Delivered Trade

The *ABLVT-GT's* sensitivity to the amount of payload delivered was investigated next. Recall the baseline mission called for 25Klbs to ISS orbit. The authors chose to examine 20 Klbs, 15 Klbs, and 10 Klbs pound options. In addition to the reduced payload mass, the payload bay volume was reduced and the corresponding volume reduction was used to increase the PEF of the vehicle. In reducing the payload volume, a constant payload density of 3.2 pcf, that corresponds to the baseline payload density, was maintained. This volume reduction also reduced the required payload bay structure weight.

Table 5 summarizes the results for the payload sweeps. As expected, the smallest payload of 10Klbs

results in the lowest GLOW and dry weight. Notice though that the reduction on dry and GLOW weight are nonlinear. For a vehicle with a GLOW of 1,000,000 lbs. (a proposed runway weight constraint), the data can be interpolated to yield a payload of 11.3 Klbs to ISS.

Table 5. Payload Sensitivity Sweeps.

Payload (Klbs)	GLOW (Klbs)	Dry (Klbs)	Mix. Ratio	Length (ft)
25	1,351	230	3.54	190.5
20	1,283	218	3.53	186.1
15	1,122	193	3.53	176.1
10	957	167	3.49	164.6

Turbine Based Combination Propulsion Trade

A turbine-based low speed propulsion system option, capable of delivering 25 Klbs to ISS, was considered next. This vehicle features an over-under propulsion system arrangement similar to the LaRC reference concept. For the high speed propulsion system, dual-mode ramjet/scramjet engines were used. A large tail rocket was added to the vehicle that had a vacuum Isp of 465 seconds and uninstalled T/W_e of 77. The vehicle used the Mach 6/10 Aerojet forebody design. The transition Mach number was increased from the baseline value to Mach 12.

Performance data for the low-speed propulsion system was generated using GECAT¹⁴. These engine were modeled as an ‘afterburning turbojet’ with a MIL-SPEC variable geometry inlet. The additional assumption was made that the engines were always operating at their design point. Specific design details were chosen to be representative of advanced turbine engine technology. The maximum engine diameter was determined by computing the available space between the high speed propulsion system and payload bay. The vehicle can contain a maximum of 7 low speed engines, each with a maximum diameter of 5 ft. at a vehicle length of 200 ft. Figure 16 shows the ratio of engine thrust to sea-level-static thrust versus Mach number at various altitude generated using GECAT.

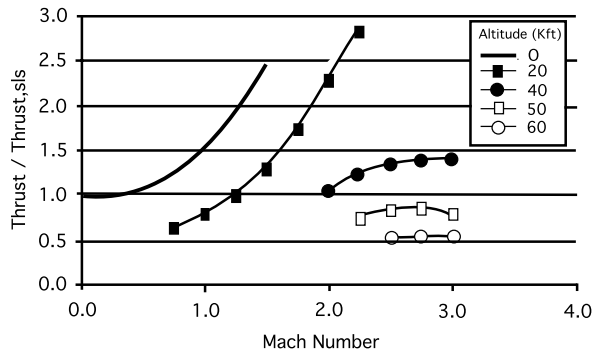


Figure 16. Low Speed Thrust Ratio vs Mach Number

A new CAD model was constructed to adjust the PEF numbers to reflect the internal fuselage volume occupied by the low speed system. PEF was decreased by approximately 3% from the baseline vehicle values for all three vehicle length scales.

For the main propulsion system weight, not including the tail rocket, installed T/W_e 's of 7.5 and 10 were examined. This weight is assumed to include all hardware for the turbine system, dual mode engine system, and low speed forebody ramp hardware. The 15% dry weight margin, added to all other subsystems, was not added to this weight. Due to poor thrust levels in the transonic regime, it was necessary to ignite the tail rocket from Mach 0.7 to Mach 1.7. Refinement of the turbine system could reduce this operating range.

Table 6. Turbine-Powered Low Speed *ABL*-*GT* Results ($M_{tr}=12$).

T/W_e	GLOW (Klbs)	Dry (Klbs)	Mix. Ratio	Length (ft)
7.5	2,120	499	1.68	239.6
10.0	1,676	389	1.68	225.5

The results for the turbine-powered low speed vehicle are presented in Table 6. With a mass ratio of 3.64, the I^* for this concept is 598 seconds. Note that for the most optimistic engine weight, the dry weight of 389 Klbs is 70% heavier than the baseline RBCC powered concept.

It appears that for these particular cases, the turbine-powered system is not a very attractive option. The authors feel that this combination propulsion system will be more suited for use as a booster of a two stage to orbit (TSTO) vehicle.

One area for future exploration will be the high-speed propulsion system design point. Scramjet transition above Mach 12 will probably be required to reduce the vehicle GLOW and dry weight, assuming significant improvement in the scramjet performance at these higher Mach numbers can be made.

Vehicle Mission Trade

The last trade conducted considered an *ABL*-*GT* vehicle designed for more commercially oriented mission. This vehicle delivers 15,000 lbs. to a final circular orbit of 100 nmi., at an inclination of 28.5 degrees, due east from KSC. For this case, the DMRJ engines were used, with a transition Mach number of 11. For the analysis of this mission scenario, the required OMS propellants were reduced to provide a total delta-V capability of 650 fps. Additionally, the payload bay volume was reduced from 7,875 ft^3 to 4,725 ft^3 .

This LEO version of the *ABL*-*GT* has a gross weight of 777,300 lbs. and a dry weight of 142,200 lbs. This is significantly lower than the baseline vehicle concept. The main design factors allowing for this weight reduction were the reduced OMS requirement, reduction of 10,000 lbs. of payload capability, and the improved propellant packaging efficiency. The authors would argue that this smaller vehicle will have shorter turnaround times and thus be able to fly more routinely than the ISS mission designs. The reduction in per flight payload capability can be counteracted with more flights, leading to a more efficient ground operations scenario. The smaller vehicle also translates into lower DDT&E costs. These upfront costs are the most significant factor in assessing a programs economic viability, assuming the DDT&E costs will be financed through loans.

FUTURE WORK

A number of areas for future study and improvement of the *ABL_V-GT* vehicle have already been identified by the authors. Some of these areas are:

- 1) dynamic pressure boundary
- 2) 'wing' incidence angle
- 3) engine bypass ratio
- 4) OML shape
- 5) LOX tank structure and materials

A few concerns with the weight model and configuration assumptions were raised by outside organizations during the course of the study. The authors do not feel that at this stage in the design process, it is possible to resolve these concerns adequately. However, in an attempt to address these issues to test weight sensitivity to certain assumptions, three additional vehicle designs were closed.

The baseline *ABL_V-GT* vehicle (25 Klbs, $M_{tr}=10$ Strutjet) was used as the starting point for this survey. The first item of concern involved the use of advanced EMAs instead of hydraulic wing actuators. Thus, hydraulic systems were added to the vehicle (MER of 0.5% of GLOW). The next item of concern involved the vehicle planform loading. With the high mixture ratio due to the RBCC engines and poor subsonic lift capability of the ABLV configuration, it had been suggested that additional wings will be required to allow acceptable takeoff speeds. So called 'auxiliary wings' were thus added to the vehicle. A simplified wing weight of 5.0 psf based solely on exposed wing area was assumed. A target vehicle planform loading value that allows for a takeoff speed under 300 knots was then set as a constraint in the W&S spreadsheet (wing area as an independent variable). The planform loading is defined as the vehicle liftoff weight divided by the fuselage planform area. The third item involved a potential increase in vehicle bending loads due to the higher mixture ratios. This 'LOX penalty' was thus added to the vehicle fuselage structural weights. The penalty was a quadratic, 1-D function of the vehicle's overall mixture ratio. Each penalty was added incrementally and the baseline *ABL_V-GT* was reclosed each time.

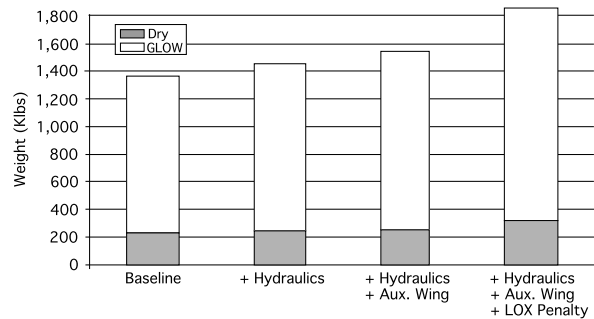


Figure 17. Cumulative Penalty Effect on Baseline *ABL_V-GT*.

Figure 17 shows the cumulative effect, on GLOW and dry weight, of adding these penalties to the baseline concept. The authors would like to point out that these effects would be less severe with increasing M_{tr} and decreasing payload size. Since the MER for each penalty is based directly on GLOW or vehicle mixture ratio, higher transition Mach numbers would be favored significantly if the engine and forebody was also redesigned for the new peak design Mach number.

SUMMARY

An airbreathing SSTO concept based on a reference ABLV concept with RBCC propulsion has been presented. The *ABL_V-GT* is a third generation RLV designed to deliver 25,000 lbs. to the International Space Station. Advanced propulsion, materials, and systems technologies are used throughout the vehicle. A collaborative, team-oriented design process was used to perform the conceptual design. For the baseline mission, the gross weight was determined to be 1,352,000 lbs., with a dry weight of 230,000 lbs.

Numerous trade studies were conducted by the *ABL_V-GT* design team. The vehicle system's sensitivity to the scramjet transition Mach number was investigated, along with an alternative engine design (DMRJ). These results suggested a 10% decrease in dry weight and 8% decrease in GLOW was achievable by increasing the transition Mach number to 11 and using the DMRJ engines, relative to the baseline design.

The *ABL_V-GT*'s sensitivity to payload weight was assessed and showed that significant reductions in

vehicle size are achievable when the payload is decreased from the baseline specification of 25,000 lbs. With a reduced payload of 11,300 lbs., a vehicle with a GLOW of 1,000,000 lbs. can be obtained.

An alternate mission scenario of 15,000 lbs payload to low Earth orbit was conducted, as well as a turbine-based combination system propulsion option carrying 25,000 lbs. to the ISS. The LEO mission vehicle resulted in a GLOW of 777,300 lbs. and dry weight of 142,200 lbs. However, the turbine-based system results were somewhat disappointing, resulting in a GLOW of 1,675,500 lbs. and dry weight of 389,200 lbs. for the very optimistic engine thrust –to-weight ratio 10.0 at a M_{tr} of 12.

Figure 18 compares four of the more interesting *ABL*V-*GT* vehicles (baseline, $M_{tr}=11$ DMRJ, $T/W=10$ TBCC, and LEO) resulting from the study, in terms of dry and gross weight.

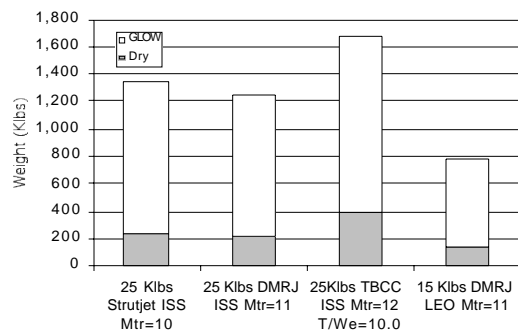


Figure 18. *ABL*V-*GT* Trades Performance Summary.

ACKNOWLEDGEMENTS

This research was supported by NASA's Marshall Space Flight Center grant number NAG8--1302 entitled "Launch Vehicle Systems Analysis" under the direction of Mr. Uwe Hueter.

The authors gratefully acknowledge the contributions of former SSDL graduate students Lt. Kris Cowart (aeroheating/TPS) and Ashraf Charania (cost) for the success of this work.

BIBLIOGRAPHY

1. Mankins, J. C., "Lower Costs for Highly Reusable Space Vehicles," *Aerospace America*, March, 1998, pp. 36 – 42.
2. Olds, J.R., Bradford, J., et al. "Hyperion: An SSTO Vision Vehicle Concept Utilizing Rocket Based Combined Cycle Propulsion." AIAA 99-4944, 9th International Space Planes and Hypersonic Systems and Technologies Conference, Norfolk, VA. November, 1999.
3. Hueter, U., and Turner, J., "Rocket-Based Combined Cycle Activities in the Advanced Space Transportation Program Office." AIAA 99-2352, 35th AIAA/ASME/SAE/ASEE Joint Propulsion Conference and Exhibit, Los Angeles, CA. June, 1999.
4. Moses, P.L., and Ferlemann, S.M., et al. "An Airbreathing Launch Vehicle Design with Turbine-Based Low-Speed Propulsion and Dual Mode Scramjet High-Speed Propulsion." AIAA 99-4948, 9th International Space Planes and Hypersonic Systems and Technologies Conference, Norfolk, VA. November, 1999.
5. Reubush, D., "Hyper-X Stage Separation – Background and Status." AIAA 99-4818, 9th International Space Planes and Hypersonic Systems and Technologies Conference, Norfolk, VA. November, 1999.
6. Sova, G., and Divan, P., "Aerodynamic Preliminary Analysis System II, Part II – User's Manual," NASA CR 182077, April, 1991.
7. Bulman, M. and Siebenhaar, A., "The Strutjet Engine: Exploding the Myths Surrounding High Speed Airbreathing Propulsion." AIAA 95-2475, 31st AIAA/ASME/SAE/ASEE Joint Propulsion Conference and Exhibit, San Diego, CA. July, 1995.
8. Siebenhaar, A., et al. "Demonstrating the Performance Benefits of the Strutjet RBCC for Space Launch Architectures." 11TH PERC symposium, November 18-19, 1999.

9. Brauer, G. L., D. E. Cornick, and Stevenson, R., "Capabilities and Applications of the Program to Optimize Simulated Trajectories," NASA CR 2770. February, 1977.
10. Olds, J. R., and Budianto, I. A., "Constant Dynamic Pressure Trajectory Simulation in POST." AIAA 98-0302, 36th Aerospace Sciences Meeting and Exhibit, Reno, NV. January, 1998.
11. Engel, C. D., and Konishi, S., "MINIVER Upgrade for the AVID System," NASA CR 172213, August, 1993.
12. NASA Ames Thermal Protection Materials and Systems Branch, TPS-X Database Internet Site, <http://asm.arc.nasa.gov>.
13. Cowart, K., and Olds, J., "Integrating Aeroheating and TPS into Conceptual RLV Design." AIAA 99-4806, 9th International Space Planes and Hypersonic Systems and Technologies Conference, Norfolk, VA. November 1-5, 1999.
14. DePlachett, C, "Application of the GECAT Software for Instruction in Gas Turbine Propulsion Analysis." AIAA 2000-3893, 36th AIAA/ASME/SAE/ASEE Joint Propulsion Conference and Exhibit, Huntsville, AL. July, 2000.